SUPPLEMENTARY INFORMATION

Vibrio cholerae FruR facilitates binding of RNA polymerase to the *fru* promoter in the presence of fructose 1-phosphate

Chang-Kyu Yoon[1], Deborah Kang[1], Min-Kyu Kim[2] and Yeong-Jae Seok[1]

[1] School of Biological Sciences and Institute of Microbiology, Seoul National University, Seoul, 08826, Korea.

[2] Radiation Research Division, Korea Atomic Energy Research Institute, Jeongeup, 56212, Korea.

*To whom correspondence should be addressed. Tel: +82 2 880 4414; Fax: +82 2 871 1993; Email: yjseok@snu.ac.kr.

SUPPLEMENTARY MATERIALS AND METHODS

Primer extension analysis

Primer extension analysis using a hexachlorofluorescein (HEX)-labeled primer was carried out as previously described (1) with some modifications. To identify the transcription start site (TSS) of *fruB*, HEX-labelled primer (Bionics, Korea) (50 pmol) which anneals to the region from -151 to -170 relative to the initiation codon of *fruB* was used (Supplementary Table 2). Total RNA (150 μg) extracted from wild-type *V. cholerae* N16961 cells grown on fructose or glucose was mixed with the primer in hybridization buffer (40 mM PIPES, pH 6.5, 400 mM NaCl and 1 mM EDTA), denatured at 95°C for 5 min, and hybridized at 52°C for 6 h. Reverse transcription was performed using RevertAid reverse transcriptase (Thermo Fisher Scientific, Inc., Waltham, MA, USA, #EP0441) in the presence of RNaseOUT (Invitrogen, Carlsbad, CA, USA, #10777-019). DNA and RNA were collected through phenol extraction and ethanol precipitation. HEX-labeled products and aliquots of sequencing reaction were analysed by capillary electrophoresis in an ABI 3730xl DNA analyzer (Applied Biosystems, Foster City, CA) with Peak Scanner software v1.0 (Applied Biosystems, Foster City, CA).

Primer extension analysis using a [γ-^{32}P]ATP-labeled primer was carried out as previously described (2) with some modifications. To identify the TSS(s) of *fruR*, the primer which anneals to the region from +90 to +70 relative to the initiation codon of *fruR* (15 pmole) (Supplementary Table 2) was incubated with 1 unit of T4 polynucleotide kinase (NEB) in the presence of 30 μCi of [γ-^{32}P] ATP at 37°C for 1 h and the [γ-^{32}P]ATP-labeled primer was purified using ProbeQuant™ (GE Healthcare Life Sciences). Total RNA (150 μg) extracted from wild-type *V. cholerae* N16961 cells grown on fructose was mixed with the primer in hybridization buffer, denatured at 95°C for 5 min and hybridized at 52°C for 6 h. Reverse

transcription was performed using RevertAid reverse transcriptase in the presence of RNaseOUT. DNA and RNA were collected through phenol extraction and ethanol precipitation. The [γ-^{32}P] ATP-labeled products and aliquots of sequencing reaction were resolved on a 5% denaturing polyacrylamide gel (acrylamide/bisacrylamide ratio of 19:1) in TBE. The sequencing ladders were generated using a Thermo Sequence Cycle Sequencing kit (USB) using the *V. cholerae* N16961 chromosome as a template with the same primers used in the annealing procedure.

$KMnO_4$ footprinting

KMnO4 footprinting analysis using a HEX-labeled probe was carried out as previously described (3), with some modifications. The HEX-labeled on the non-template strand encompassing -109~+24 was generated by PCR using the appropriate primer sets (Supplementary Table 2). The DTT was eliminated from the buffer containing the proteins by dialysis. The DNA probe (200 ng) was incubated with VcFruR (650 ng) or hybrid RNAP (EcCore 0.7 μg and *V. cholerae* σ70 1.4 μg) in the presence or absence of F1P (2 mM) for 10 min at 37˚C in a buffer containing (10 mM Tris-HCl, pH 8.0; 100 mM KCl; 10 mM $MgCl_2$, and 0.1 μg/μl BSA), then treated with $KMnO_4$ (2.5 mM) for 2 min at 37˚C. Reactions were stopped by the addition of β-mercaptoethanol (0.34 M) and precipitated with 0.3 M sodium acetate and ethanol. Then, DNA was precipitated again with 2 M ammonium acetate and ethanol. After the pellet was air dried, 100 μl 1 M piperidine was added and incubated at 90˚C for 30 min. Samples were precipitated with sodium acetate and ethanol and were analyzed by capillary electrophoresis in an ABI 3730xl DNA Analyzer (Applied Biosystems, Foster City, CA) with Peak Scanner software v1.0 (Applied Biosystems, Foster City, CA)

SUPPLEMENTARY FIGURES

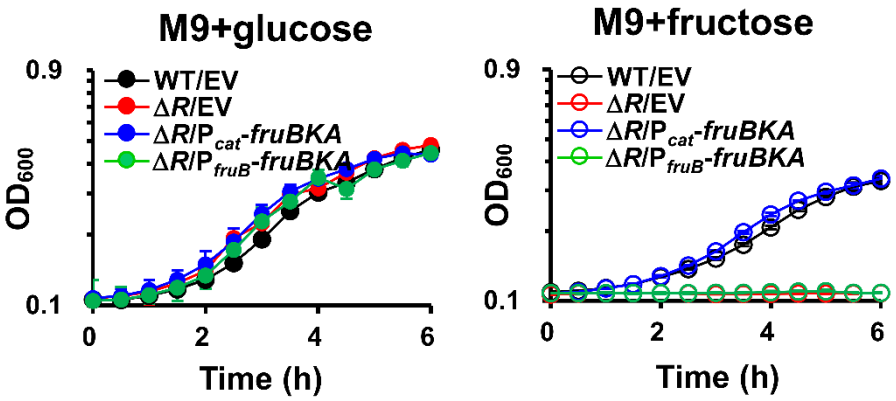

Supplementary Figure 1. FruR-independent expression of *fruBKA* operon cannot rescue the growth defect of Δ*fruR* on fructose

Comparison of the growth of the wild type and *fruR* mutant harboring a plasmid carrying a *fruBKA* operon under control of its own promoter (P_{fruB}-*fruBKA*) or the constitutive *cat* promoter (P_{cat}-*fruBKA*) on glucose and fructose. The means and standard deviations of three independent measurements are shown. EV, empty vector.

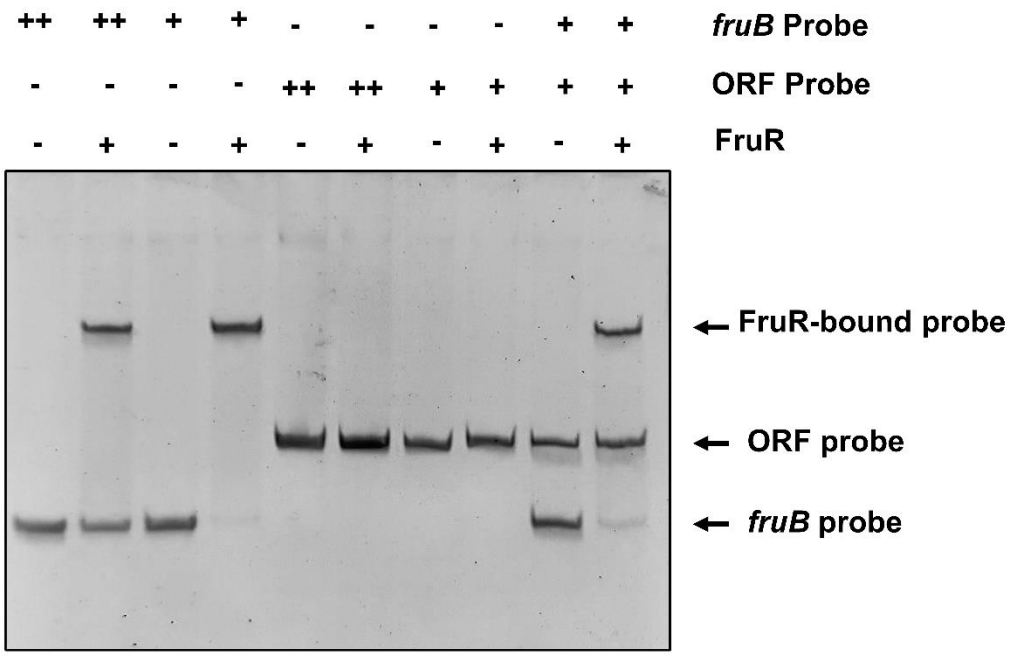

Supplementary Figure 2. Specific binding of FruR to the *fruB* promoter.

An EMSA competition assay was conducted to confirm the specific binding of FruR to the *fruB* promoter using a DNA fragment from the *fruB* ORF as a competitor. The 438-bp ORF probe encompassing +121 to +618 relative to the initiation codon of *fruB* was generated using the primer pair of B-ORF-F and B-ORF-R (Supplementary table 2). Each probe (30 or 60 ng) was incubated with VcFruR (120 ng) and analysed on a 6% polyacrylamide gel in TBE as described under “Materials and methods”.

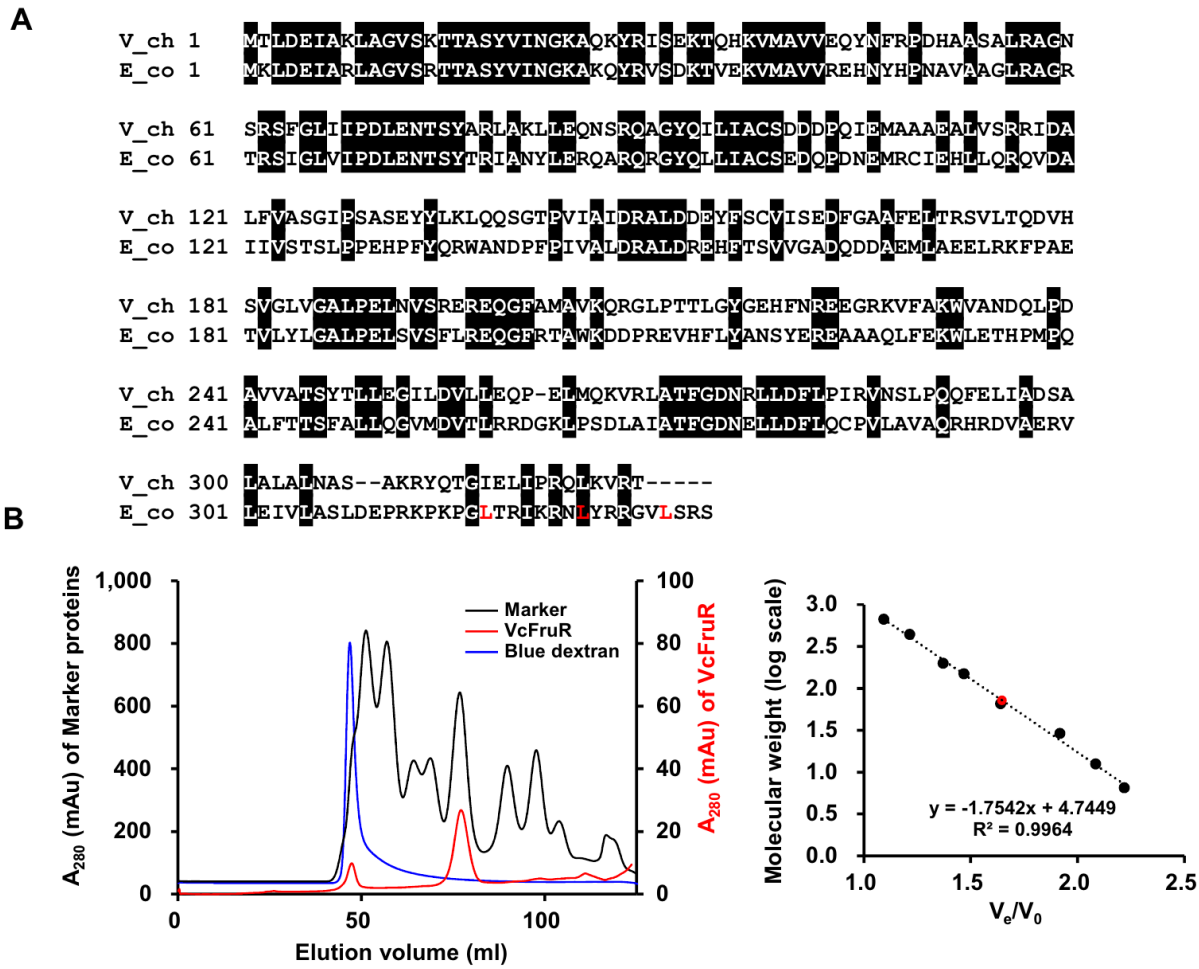

Supplementary Figure 3. Determination of the oligomeric state of VcFruR.

(A) Amino acid sequence alignment of FruRs from *E. coli* (E_co) and *V. cholerae* (V_ch) using ClustalX2 software. Conserved amino acids between two FruR orthologs are shaded in black and leucine-mini-zipper sequences are colored in red. **(B)** Molecular weight (MW) determination of VcFruR by gel filtration chromatography. Samples were applied to an XK 16/60 column manually packed with Superdex 200 prep grade and eluted in 50 mM Tris-HCl, pH8.0, containing 200 mM NaCl, 10 mM DTT, 10 mM EDTA and 10% glycerol at a flow rate of 1.5 ml/min using a FPLC system (GE Healthcare Life Sciences), and protein elution was monitored at 280 nm. The column was calibrated using MW markers from Sigma-Aldrich (black curve) and the void volume (V_0) was determined from the elution of blue dextran (MW ~ 2,000 kDa, blue curve). The elution profile of VcFruR is shown in red (left

panel). From the plot of log(MW) versus the V_e/V_0 value (right panel), where V_e is the elution volume of each protein, the MW of VcFruR was estimated to be 71.82 kDa (red dot), supporting its existence as a dimer in solution (monomer ~ 36.817 kDa). MW markers: Thyroglobulin (669 kDa), Apoferritin (443 kDa), β-amylase (200 kDa), Alcohol dehydrogenase (150 kDa), Albumin (66 kDa), Carbonic anhydrase (29 kDa), Cytochrome C (12.5 kDa), and Aprotinin (6.5 kDa).

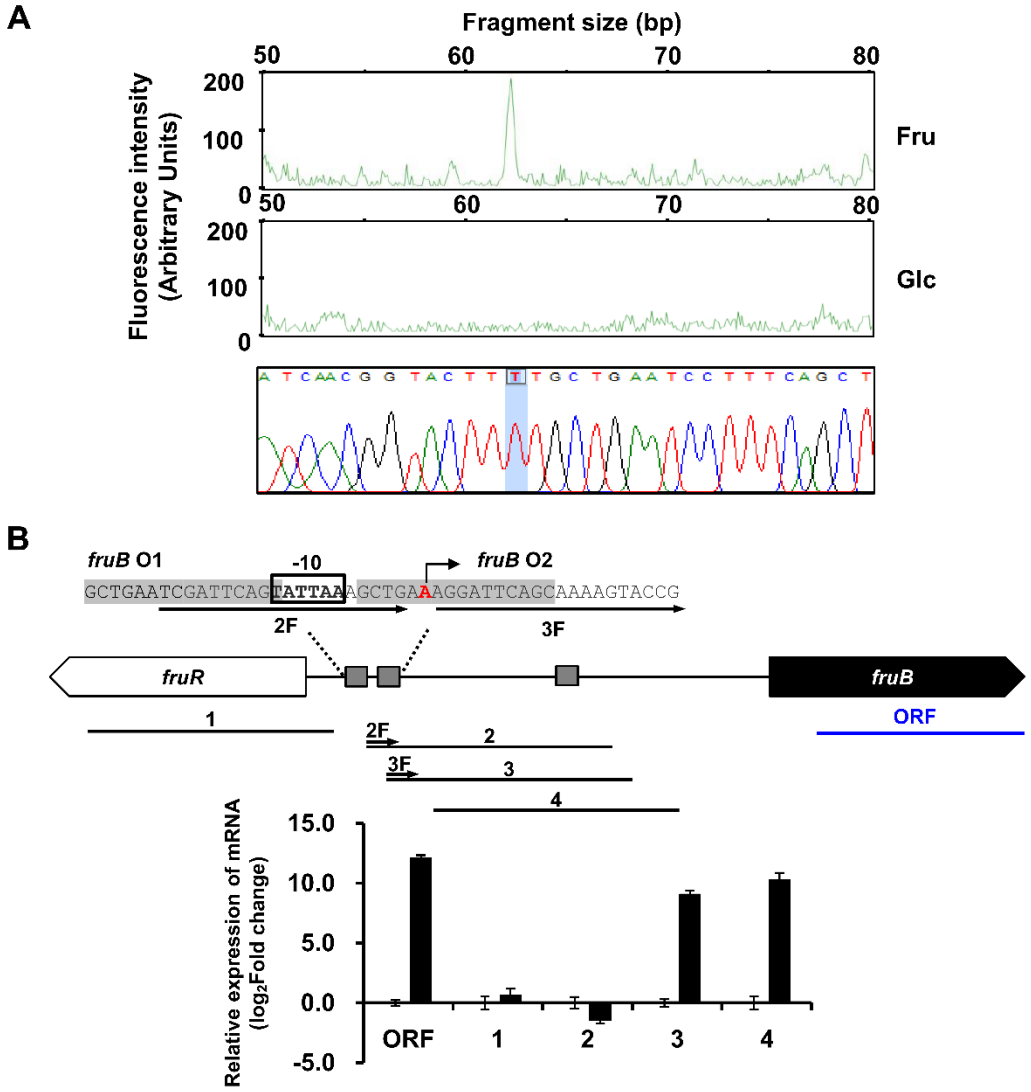

Supplementary Figure 4. Identification of the *fruB* transcription start site (TSS).

(A) Mapping the TSS of *fruB* by primer extension. Primer extension analysis was performed using a hexachloro-fluorescein (HEX)-labeled primer and the total RNA extracted from wild-type (WT) *V. cholerae* N16961 cells grown on fructose (Fru) as a template as described under "Supplementary Materials and Methods". Primer extension product using the same primer and the total RNA extracted from the same strain grown on glucose (Glc) as a template was used as a control. The sequencing ladder and corresponding reverse-complementary nucleotide sequence are shown below. The nucleotide corresponding to the peak observed only in the primer extension product using the RNA extracted from the cells grown on

fructose was determined as the TSS (marked with box and shaded in blue). Fragment sizes were determined by comparison to the internal molecular weight standards **(B)** Fructose-dependent transcription from the TSS was further confirmed by RT-PCR. The FruR-binding sites are depicted by grey rectangles and nucleotide sequences corresponding to *fruB* O1 and O2 are shaded in grey. The TSS of *fruB* is colored in red with a bent arrow and the -10 element is boxed. The RT-PCR reactions designed to determine the *fruB* TSS are schematically shown by the lines with numbers and the RT-PCR reaction of the *fruB* ORF served as a positive control is depicted by a blue line. The forward primers used for amplification of single RNA molecules encompassing regions 2 or 3 are indicated with arrows under the nucleotide sequence (2F and 3F, respectively) (Supplementary Table 2). The amount of each RT-PCR product using RNA isolated from cells grown on fructose as a template (filled bars) are shown as $\log_2$ values relative to those using RNA from cells grown on glucose as a template (open bars) (lower panel).

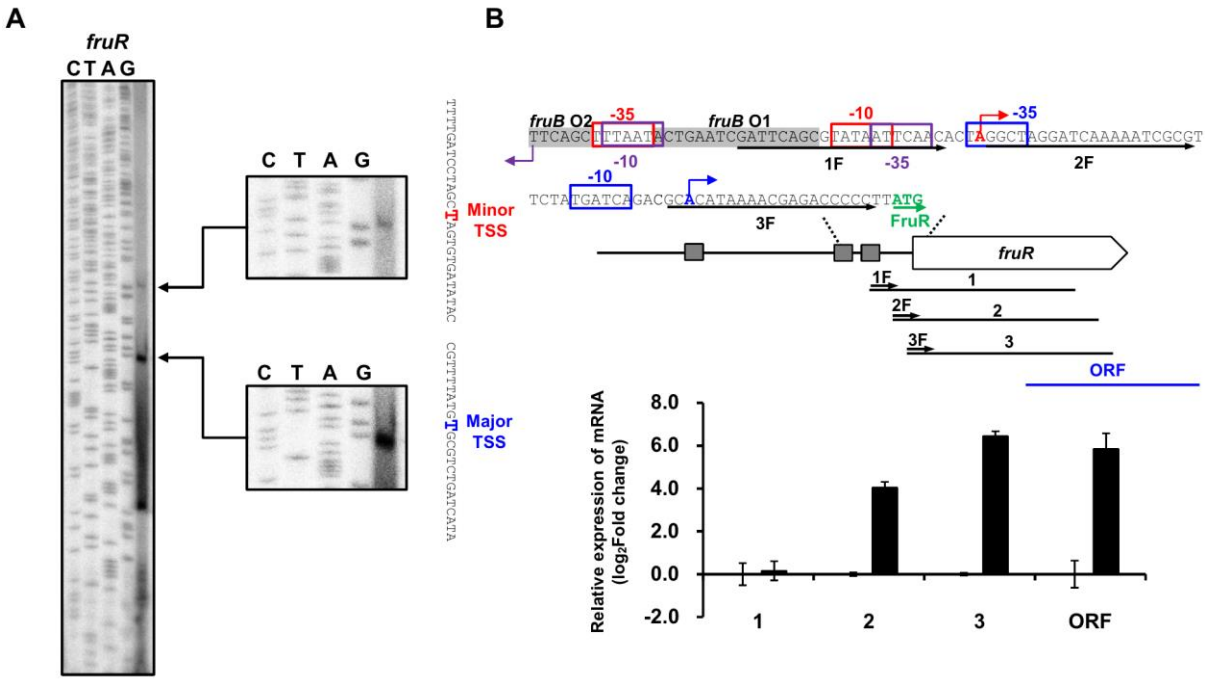

Supplementary Figure 5. Identification of the TSS(s) of *fruR*.

(A) Identification of the TSS(s) of *fruR*. (A) Mapping the TSS(s) of *fruR* by primer extension. Primer extension analysis was performed using the total RNA extracted from WT N16961 cells grown on fructose with a [γ-^{32}P] ATP-labeled primer, as described under "Supplementary Materials and Methods". Lanes C, T, A and G contain each dideoxy sequencing product. Corresponding reverse-complimentary nucleotide sequences are shown and the minor and major TSSs are colored in red and blue, respectively, in a larger font size (right). **(B)** Fructose-dependent transcription from the TSSs was further confirmed by RT-PCR. The FruR-binding sites are depicted by grey rectangles and nucleotide sequences corresponding to *fruB* O1 and O2 are shaded in grey. The initiation codon of *fruR* is colored in green and marked with an arrow. Two TSSs of *fruR* are indicated with bent arrows, with their -35 and -10 elements boxed in red and blue colours, respectively. The TSS and -35 and -10 elements of the *fru* operon, which is divergently transcribed from *fruR*, are indicated with a bent arrow and boxes in purple colour, respectively. The RT-PCR reactions designed to confirm the *fruR* TSS are schematically shown by the numbered lines, while the RT-PCR

reaction of the *fruR* ORF serving as a positive control is depicted by a blue line. The forward primers used for amplification of single RNA molecules are indicated with arrows under their respective nucleotide sequence (#F). The amounts of each RT-PCR product using RNAs isolated from cells grown on fructose as a template (filled bars) are shown as $\log_2$ values relative to those using RNAs from cells grown on glucose as a template (open bars) (lower panel).

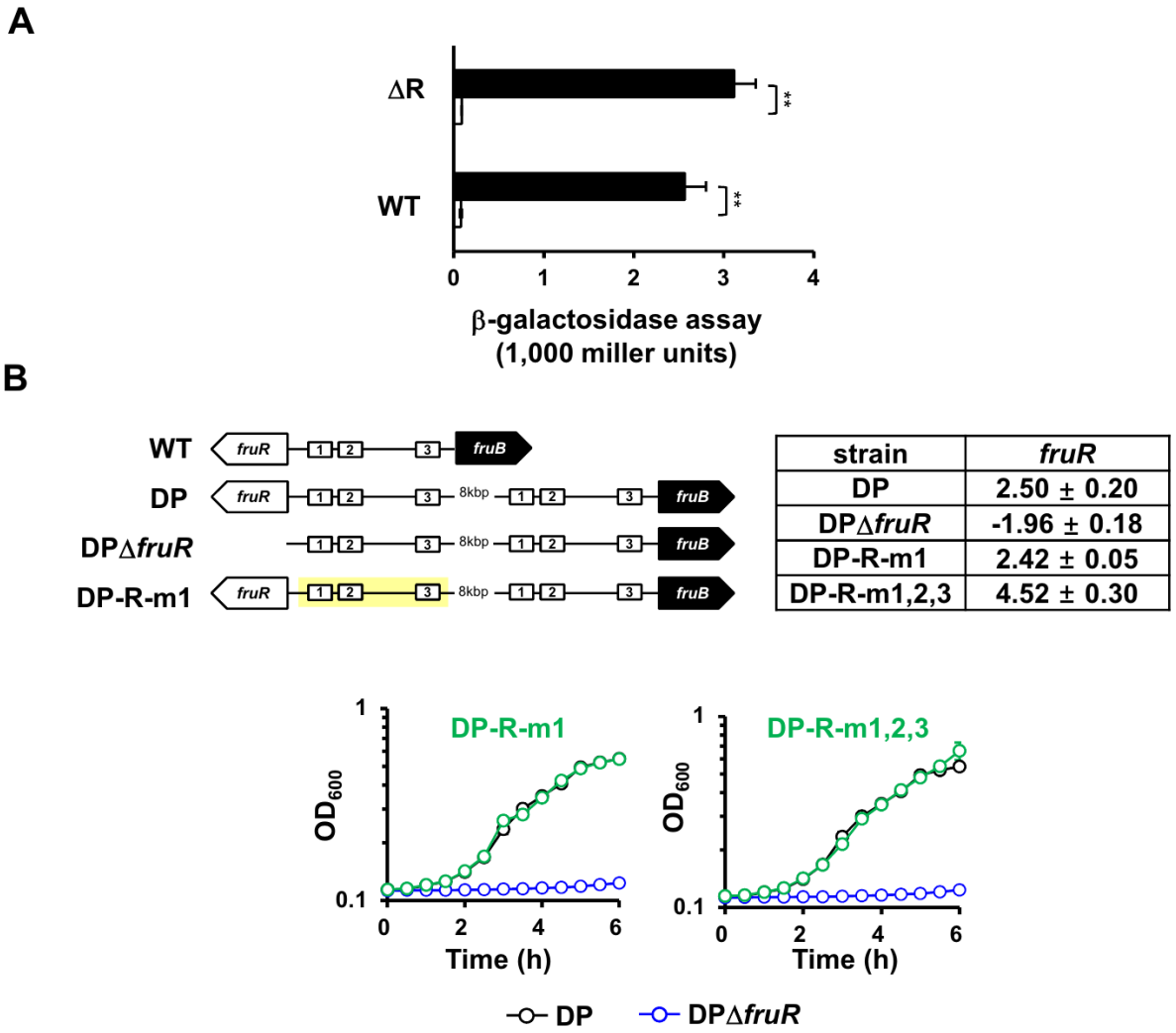

Supplementary Figure 6. Binding of FruR to operators is not involved in the transcriptional activation of *fruR*.

(A) Effect of the presence of VcFruR on the fructose-induced transcriptional activation of *fruR* was examined by the *lacZ* reporter assay using *fruR*$^{+}$ *lacZ*$^{-}$ (WT) and *fruR*$^{-}$ *lacZ*$^{-}$ (ΔR) strains harboring the plasmid carrying *E. coli lacZ* transcriptionally fused with the wild-type *fruR* promoter. Both strains were grown on glucose (open bars) or fructose (filled bars) and then lysed to measure the β-galactosidase activity as described under "Materials and Methods." Statistical significance was determined using the Student's *t*-test. (**P<0.01) **(B)** Effect of VcFruR binding to operators on *fruR* transcription was examined using fructose-grown strains carrying the chromosomal duplication of the wild-type or mutated *fruR-fruB*

intergenic sequence. Schematic representation of the strains carrying the chromosomal duplication of the *fruR-fruB* intergenic region is shown in the upper left panel, with wild-type FruR-binding sites and mutated areas depicted by white rectangles and yellow shadings, respectively. The mRNA expression levels of *fruR* in the indicated strains grown on fructose were analyzed using qRT-PCR and shown as $\log_2$ values relative to that in the DP strain grown on glucose (upper right panel). Growth of DP-R-m1 and DP-R-m1,2,3 strains on fructose was compared with the DP (black) and DPΔ*fruR* (blue) strains (lower panel). Means and standard deviations of three independent measurements are shown in **(A)** and **(B).**

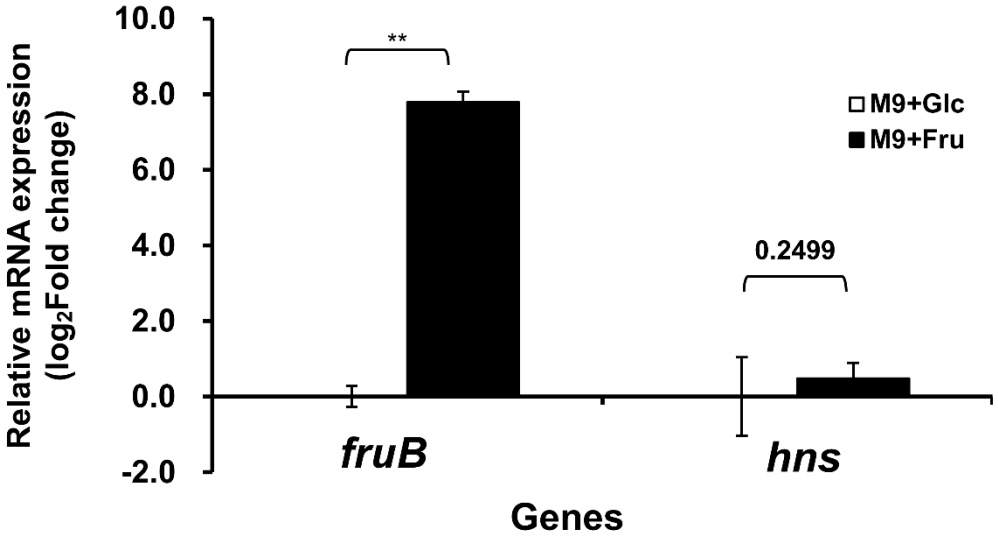

Figure 7. The transcriptional level of *hns* (VC1130) was not significantly affected by the presence of fructose

The relative mRNA expression of *fruB* and *hns* in the wild-type *V. cholerae* N16961 grown on glycerol, glucose and fructose. The mRNA expression levels of genes are shown as relative values (log_2 scale) to that of the cells grown on glycerol. The means and standard deviations of three independent measurements are shown. Statistical significance was determined using the Student's *t*-test. ($P > 0.05$ was presented, $^{**}P<0.01$)

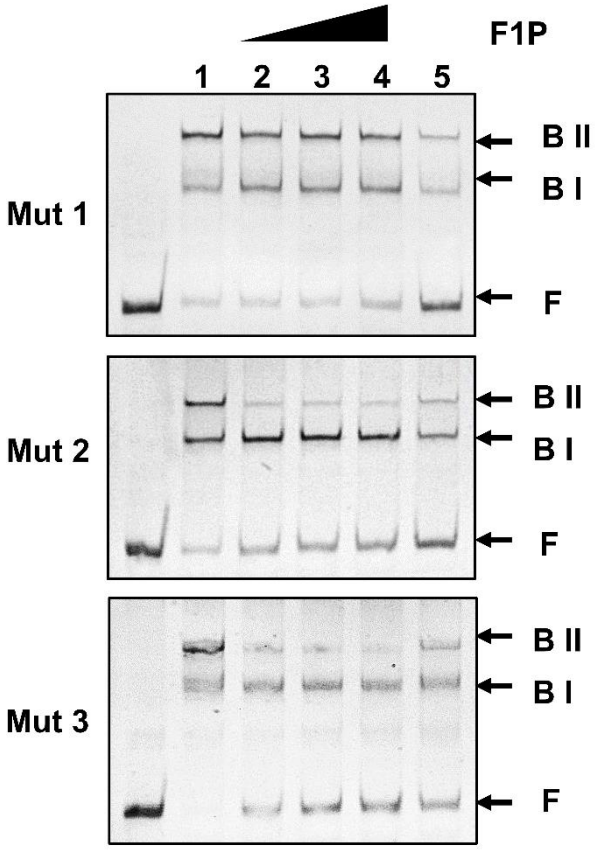

Supplementary Figure 8. F1P weakens the binding affinity of VcFruR for *fruB* O1.

The 338-bp *fruB* probes (60 ng) containing two wild-type and one mutated binding sites (mutated site indicated as Mut #) were incubated with VcFruR (60 ng) in the presence of increasing concentrations of F1P (0, 0.5, 1 and 2 mM in lanes 1-4, respectively) and resolved on a 6% polyacrylamide gel in TBE. Lane 5 contained 30 ng of VcFruR in the absence of F1P as a control. Shifted bands (BI and BII) and free probe (F) are indicated with arrows

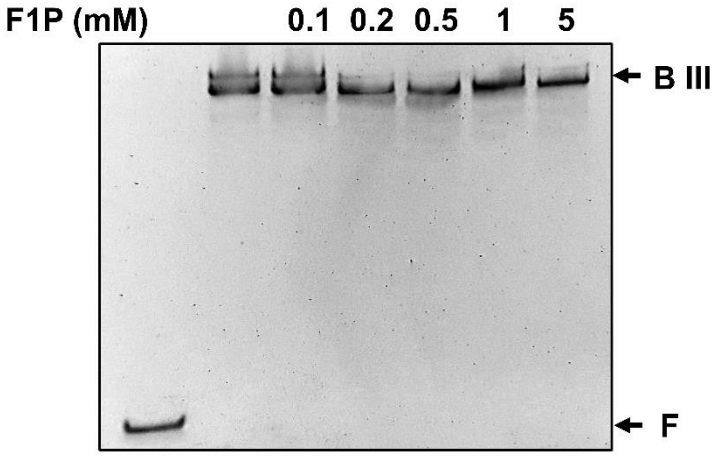

Supplementary Figure 9. F1P does not release VcFruR from the operators at the physiological ratio of VcFruR to DNA

Effect of F1P on FruR binding to the *fru* promoter in the presence of an 18-fold molar excess of FruR to DNA. The 338-bp *fruB* probe (60 ng) was incubated with FruR (360 ng) and increasing concentrations of F1P (0~5 mM as indicated) in TGED buffer and resolved on a 6% polyacrylamide gel in TBE. The shifted band (BIII) and free probe (F) are indicated with arrows.

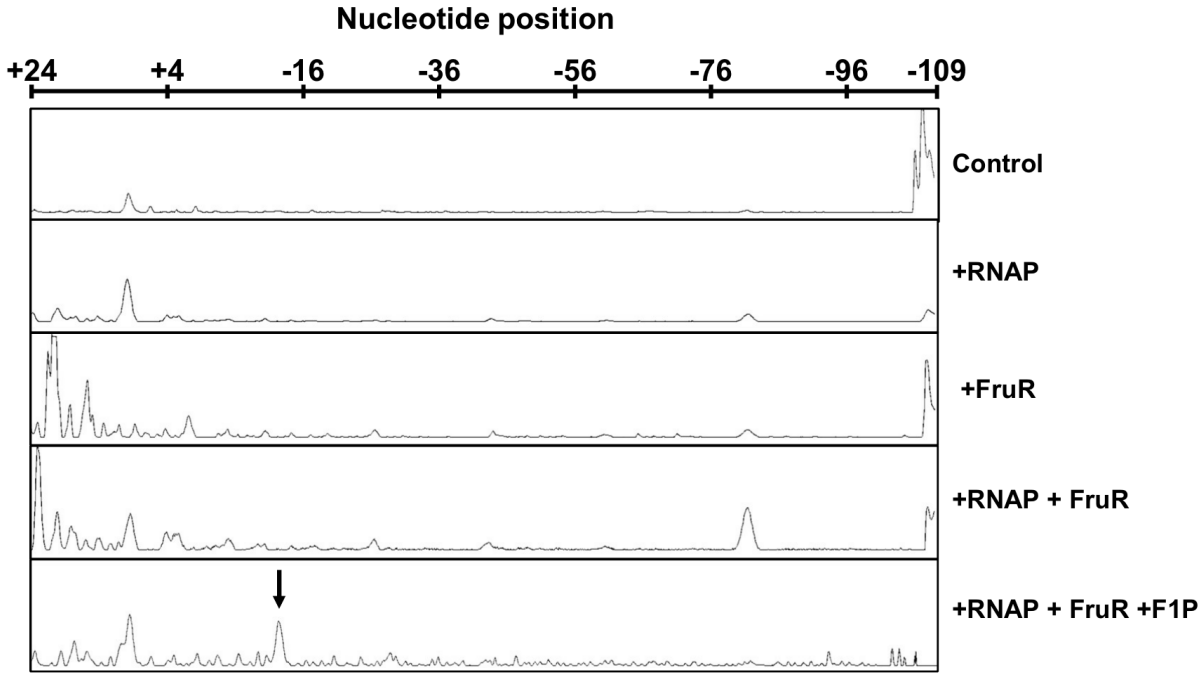

Supplementary Figure 10. VcFruR-F1P complex facilitates the open complex formation. $KMnO_4$ footprinting was conducted to examine the effect of the VcFruR-F1P complex on the open complex formation of RNAP, as described under "Supplementary Materials and Methods". The thymine positioned at -10 exhibited a strong $KMnO_4$ reactivity in the presence of both RNAP and the VcFruR-F1P complex (indicated with black arrows). Fragment sizes were determined by comparison to the internal molecular weight standards and nucleotide positions relative to the TSS are indicated.

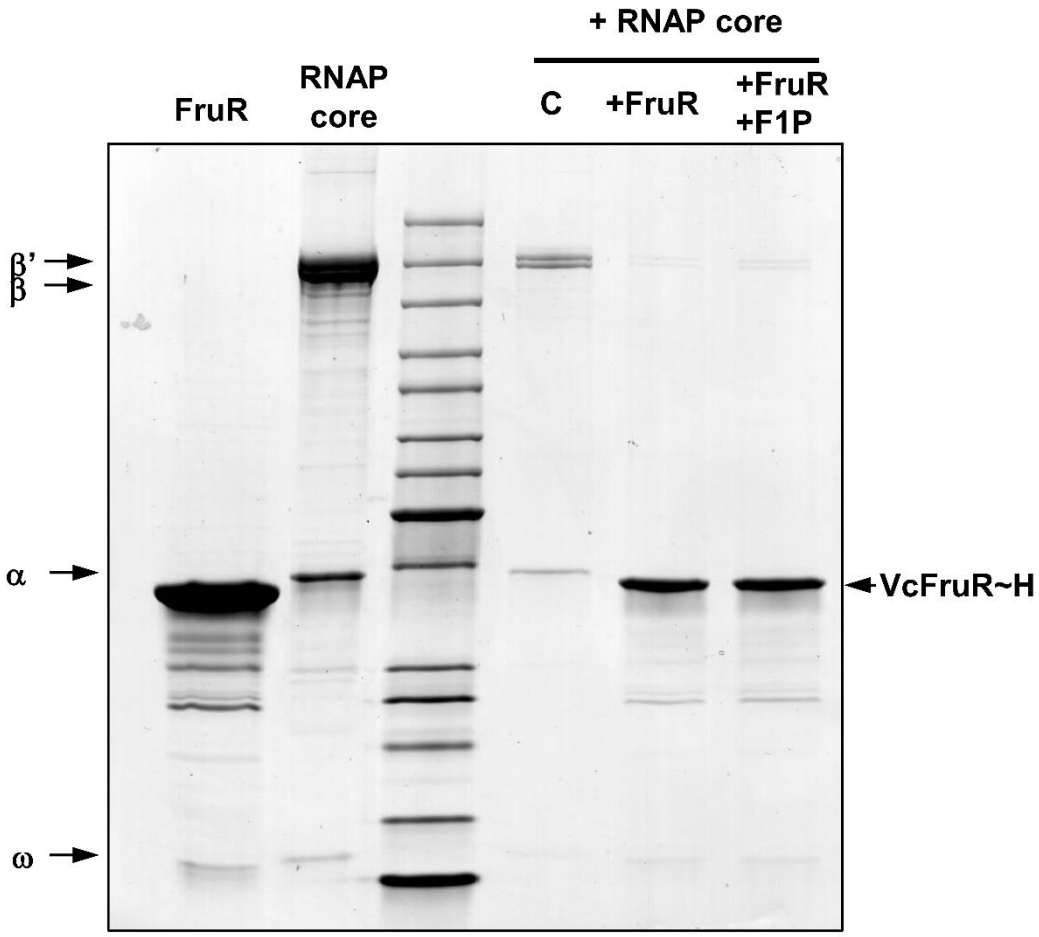

Supplementary Figure 11. Determination of the direct interaction between VcFruR and RNA polymerase subunits.

Protein affinity pull-down assay was conducted to examine the interaction between VcFruR and RNA polymerase core enzyme (RNAP). *E. coli* RNAP was mixed with buffer or His-tagged VcFruR (VcFruR-H) in the presence or absence of F1P. The samples were subjected to TALON affinity chromatography and proteins bound to the column were analyzed by SDS–PAGE using a 4–20% gradient Tris–glycine gel (KOMA biotech) and staining with Coomassie brilliant blue R. “FruR” and “RNAP core” lanes represent proteins before the pull-down experiment, respectively.

SUPPLEMENTARY TABLES

Table S1. Bacterial and plasmids used in this study.

Strains or plasmids	Genotypes and/or Descriptions	References or Source
Strains		
Vibrio cholerae		
O1 El Tor N16961	Wild type, Clinical strain	
Δ*fruR*	N16961 Δ*fruR*	This study
Δ*fruB*	N16961 Δ*fruB*	This study
Δ*fruK*	N16961 Δ*fruK*	This study
Δ*fruA*	N16961 Δ*fruA*	This study
Δ*lacZ*	N16961 Δ*lacZ*	Lab stock
Δ*lacZ fruR*	N16961 Δ*lacZ fruR*	This study
Escherichia coli		
ER2566	F^- λ^- *fhuA2* [*lon*] *ompT lacZ*::T7 gene 1 *gal sulA*11 Δ(*mcrC-mrr*)114::IS10 R(*mcr*-73::miniTn10-TetS)2 R(*zgb*-210::Tn10) (TetS) *endA1* [*dcm*]	New England Biolabs
BL21/pLysSRARE	F^- *ompT gal dcm lon hsdSB*(rB- mB-) λ (DE3) pLysSRARE(Cm^r)	Novagen
SM10/λpir	*thi thr leu tonA lacY supE recA*::RP4-2-Tc::Mu (λpir R6K) Km^r	(4)
Plasmids		
pDM4	Suicide vector for homologous recombination into *V. cholerae* chromosome, OriR6K, Cm^r	(5)
pET43.1a		Novagen
pJK1113	pBAD24 with *oriT* of RP4 and *nptI*, P_{BAD}; Km^r, Amp^r	(6)
pACYC-184	A low copy number cloning vector; Cm^r Tet^r	(7)
pDM4-*fruR*	pDM4-based suicide vector for deletion of *fruR*, Cm^r	This study
pDM4-*fruB*	pDM4-based suicide vector for deletion of *fruB*, Cm^r	This study
pDM4-*fruK*	pDM4-based suicide vector for deletion of *fruK*, Cm^r	This study
pDM4-*fruA*	pDM4-based suicide vector for deletion of *fruA*, Cm^r	This study
pDM4-DP-B	pDM4-based homologous recombination vector for chromosomal duplication of the *fruR-fruB* intergenic region on *fruB*-side, Cm^r	This study
pDM4-DP-B-m1	pDM4-DP-B-based vector containing *fruB* promoter having the mutated *fruB* O1, Cm^r	This study
pDM4-DP-B-m2	pDM4-DP-B-based vector containing *fruB* promoter having the mutated *fruB* O2, Cm^r	This study
pDM4-DP-B-m3	pDM4-DP-B-based vector containing *fruB* promoter having the mutated *fruB* O3, Cm^r	This study

pDM4-DP-B-m1,2	pDM4-DP-B-based vector containing *fruB* promoter having the mutated *fruB* O1 and O2, Cm^r	This study
pDM4-DP-B-m1,3	pDM4-DP-B-based vector containing *fruB* promoter having the mutated *fruB* O1 and O3, Cm^r	This study
pDM4-DP-B-m2,3	pDM4-DP-B-based vector containing *fruB* promoter having the mutated *fruB* O2 and O3, Cm^r	This study
pDM4-DP-B-m1,2,3	pDM4-DP-B-based vector containing *fruB* promoter having the mutated *fruB* O1, O2 and O3, Cm^r	This study
pDM4-DP-R	pDM4-based homologous recombination vector for chromosomal duplication of the *fruR-fruB* intergenic region on *fruR*-side, Cm^r	This study
pDM4-DP-R-m1	pDM4-DP-R-based vector containing *fruB* promoter having the mutated *fruB* O1, Cm^r	This study
pDM4-DP-R-m1,2,3	pDM4-DP-R-based vector containing *fruB* promoter having the mutated *fruB* O1, O2 and O3, Cm^r	This study
pJK-LacZ	pJK1113-based expression vector containing promoter-less LacZ, Amp^r	(8)
pJK-P_{fruB}::LacZ	pJK1113-based expression vector for LacZ under control of *fruB* promoter, Amp^r	This study
pJK-$P_{fruB\ m1}$::LacZ	pJK-P_{fruB}::LacZ based expression vector containing *fruB* promoter having mutated *fruB* O1, Amp^r	This study
pJK-$P_{fruB\ m2}$::LacZ	pJK-P_{fruB}::LacZ based expression vector containing *fruB* promoter having mutated *fruB* O2, Amp^r	This study
pJK-$P_{fruB\ m3}$::LacZ	pJK-P_{fruB}::LacZ based expression vector containing *fruB* promoter having mutated *fruB* O3, Amp^r	This study
pJK-$P_{fruB\ m1,2}$::LacZ	pJK-P_{fruB}::LacZ based expression vector containing *fruB* promoter having mutated *fruB* O1 and O2, Amp^r	This study
pJK-$P_{fruB\ m1,3}$::LacZ	pJK-P_{fruB}::LacZ based expression vector containing *fruB* promoter having mutated *fruB* O1 and O3, Amp^r	This study
pJK-$P_{fruB\ m2,3}$::LacZ	pJK-P_{fruB}::LacZ based expression vector containing *fruB* promoter having mutated *fruB* O2 and O3, Amp^r	This study
pJK-$P_{fruB\ m1,2,3}$::LacZ	pJK-P_{fruB}::LacZ based expression vector containing *fruB* promoter having mutated *fruB* O1, O2 and O3	This study
pJK-P_{fruB} Δ4::LacZ	pJK-P_{fruB}::LacZ based expression vector containing *fruB* promoter having 2bp deletion	This study

	in the spacer region between promoter elements	
pJK-P_{fruB} Δ2::LacZ	pJK-P_{fruB}::LacZ based expression vector containing *fruB* promoter having 2bp deletion in the spacer region between promoter elements	This study
pJK-P_{fruR}::LacZ	pJK1113-based expression vector for LacZ under control of *fruR* promoter, Amp^r	This study
pACYC-FruR	pACYC-based FruR expression vector under control of constitutive P_{cat} promoter	This study
pACYC-FruR(N73D)	pACYC-based FruR(N73D) expression vector under control of constitutive P_{cat} promoter	This study
pACYC-FruR(R197E)	pACYC-based FruR(R197E) expression vector under control of constitutive P_{cat} promoter	This study
pACYC-*fruBKA*	pACYC-based *fru* operon expression vector under control of constitutive P_{cat} promoter	This study
pACYC-P_{fruB}-*fruBKA*	pACYC-based *fru* operon expression vector under control of its own promoter	This study
pET43.1a-FruR	pET43.1a-based expression vector for FruR, Amp^r	This study
pET-RpoD	pET43.1a-based expression vector for RpoD, Amp^r	Lab stock

Table S2. Oligonucleotides used in this study.

Name	Nucleotides sequence (5'-3')	Uses
fruR-d1F	AAAAAACTCGAGTTTGCCGTAGTGACGATCG (XhoI)	Construction of pDM4-based vector for in-frame deletion
fruR-d1R	CCTTTATTTTGTAAGGGGGTCTCGTTTTATG	
fruR-d2F	CGAGACCCCCTTACAAAATAAAGGTATG	
fruR-d2R	TTTTTTAGATCTGGATAAACCTGACGCAGC (BglII)	
fruB-d1F	AAAAAACTCGAGCGATGCGGCATGATCCGGCC (XhoI)	
fruB-d1R	TTTTTTCCATGGTCTTAACTCCTGTCTGCCTC (NcoI)	
fruB-d2F	AAAAAACCATGGGGGGCATCACATGACAAAAAA AG (NcoI)	
fruB-d2R	TTTTTTTCTAGACTTTTTTATTCATGCTGCGC (XbaI)	
fruK-d1F	AAAAAACTCGAGGTGTAATGACGTCCATCAGC (XhoI)	
fruK-d1R	TTTTTTGGATCCGTGATGCCCCTTAACCTTCG (BamHI)	
fruK-d2F	AAAAAAGGATCCGGACAGAAGGTCGTGAAGATG (BamHI)	
fruK-d2R	TTTTTTTCTAGACCACGCGTTTCAACTTTGATC (XbaI)	
fruA-d1F	AAAAAACTCGAGAACTGCGCAGCATGAATAAA (XhoI)	
fruA-d1R	TTTTTTCCATGGGACCTTCTGTCCTTAGGCAC (NcoI)	
fruA-d2F	AAAAAACCATGGTCTGAGTGCATGGTGAAAGG (NcoI)	
fruA-d2R	TTTTTTTCTAGAGACAACATTCGCAGTGAGGAG (XbaI)	
B-DP-F	AGTGTCATCTCGAGAAGGGGGTCTCGTTTTATG (XhoI)	Construction of pDM4-B-DP
B-DP-R	CACAATGGGGGCCCTTTGCCGTAGTGACGATCG (ApaI)	
R-DP-F	CACGGTTACTCGAGAAATGCTCACCATAACCTAG (XhoI)	Construction of pDM4-R-DP
R-DP-R	AGTTCTAAGGGCCCCATTCTTAACTCCTGTCTGC C(ApaI)	
BZ-F	AAAAAAGTCGACAAGGGGGTCTCGTTTTATGTG(SalI)	Construction of pJK-P_{fruB}::LacZ
BZ-R	TTTTTTGTCGACTCTTAACTCCTGTCTGCCTC(SalI)	
RZ-F	TTTTTTGTCGACTCTTAACTCCTGTCTGCCTC(SalI)	Construction of pJK-P_{fruR}::LacZ
RZ-R	AAAAAAGTCGACAAGGGGGTCTCGTTTTATGTG	
Mut 1-F	TGAATTATACAGATCGTGAGTATTCGATTAAAGC TGAAAGGATTCAGCAAAAGTACCG	Introduction of mutated

Mut 1-R	CAGCTTTAATCGAATACTCACGATCTGTATAATT CAACACTAGGCTAGGATCAAAAATCG	sequence into *fruR-fruB* intergenic region
Mut 2-F	CAGTATTAAAAGATCGTGAGTATTCGAAAAGTA CCGTTGATTCACAATCTCGTC	
Mut 2-R	CGGTACTTTTCGAATACTCACGATCTTTTAATACT GAATCGATTCAGCGTATAATTC	
Mut 3-F	TGCCCTTTGTAGATCGTGAGTATTCGTCAAAGGA AAACGAGACGGGATG	
Mut 3-R	TTTCCTTTGACGAATACTCACGATCTACAAAGGG CAAAAAAATTCAGC	
Mut 1,2-F	TGAATTATACAGATCGTGAGTATTCGATTAAAAG ATCGTGAGTATTCGAAAAGTACCGTTGATTCACA ATCTCGTC	
Mut 1,2-R	GATCCTAGCCTAGTGTTGAATTATACAGATCGTG AGTATTCGATTAAAAGATCGTGAGTATTCGAAAA GTACCG	
2 del-F	GAATTATACGGAATCGATTCAGTA	
2 del-R	CGATTCCGTATAATTCAACACTAG	
4 del-F	GAATTATACGATCGATTCAGTATT	
4 del-R	ATCGATCGTATAATTCAACACTAG	
fruR-F	AAAAAACATATGACACTGG ATGAAATCGC (NdeI)	Construction of FruR expression plasmid
fruR-R	TTTTTTCTCGAGTTAAGTGCGCACCTTTAACTG (XhoI)	
pACYC-fruR-F	CCAGTGTCATTTTAGCTTCCTTAGCTCCTG	
pACYC-fruR-R	GCGCACTTAATTTTTTTAAGGCAGTTATTGGTGC	
fruR-F2	CTGCCTTAAAAAAATTAAGTGCGCACCTTTAACT	
fruR-R2	GGAAGCTAAAATGACACTGGATGAAATCGC	
N73D-F	TAATCATTCCGGATCTGGAAGACACCAGTT	
N73D-R	AAACGCGCATAACTGGTGTCTTCCAGATCC	
R197E-F	CAAACCCTTGTTCCTCTTCACGCGACACATTCA	
R197E-R	GTGTCGCGTGAAGAGGAACAAGGGTTTGCCAT	
pACYC-fru-F1	TGAGTTC TAACATTTTAGCTTCCTTAGCTCC	Construction of *fru* operon expression plasmid
pACYC-fru-R1	GGCTTCCCCATGAGTAAAGAAAAATAAGCAC	
Fru-F	TATTTTTCTTTACTCATGGGGAAGCCACTTG	
Fru-R	TAAGGAAGCTAAAATGTTAGAACTCACTACAC	
pACYC-fru-F2	ACATAAAACGAGATACGTGCCGATCAACGTC	
Fru-R2	TGATCGGCACGTATCTCGTTTTATGTGCGTC	
fruBR-E-F	TTTTGATCCTAGCCTAGTGTTGAATTATAC	EMSA probe
fruBR-E-R	TTGTCATTCATCCCGTCTCGTTTTCCTTTG	
B-ORF-F	CCGCATGGCACAACCGATACCCGTG	
B-ORF-R	AACAATCCCCCCGCAACAGCGCTCA	
fruBR-F(6FAM)	6FAM-TTTTGATCCTAGCCTAGTGTTGAATTATAC	DNase I footprinting
fruBR-LF(6FAM)	6FAM-TTGTCATTCATCCCGTCTCGTTTTCCTTTG	

rrsG-qRT-F	TTAGCCGGTGCTTCTTCTGT	qRT-PCR
rrsG-qRT-R	CAGCCACACTGGAACTGAGA	
fruR-qRT-F	AACTGAATGTGTCGCGTGAA	
fruR-qRT-R	CATCAATTCTGGCTGCTCAA	
fruB-qRT-F	GGGAACGATCACTGAGGAAA	
fruB-qRT-R	CATTGACGACTTGACCATCG	
fruK-qRT-F	GGCGTACAGGATGCGTTTAT	
fruK-qRT-R	GTGCTAGGCGCTGTAAGGTC	
fruA-qRT-F	GGAGCTCAGTAATGCCTTCG	
fruA-qRT-R	GAGAGCGCGATGATAAGACC	
1826-qRT-F	TTGCGGGTGATTTTCATACA	
1826-qRT-R	CGGTATCCCAGTTCGGTTTA	
ptsH-qRT-F	CAGAAAACGGCCTTCACACT	
ptsH-qRT-R	CGGCAGAGATAGTCACGACA	
hns-qRT-F	GCACGCGAACTGACTATTGA	
hns-qRT-R	TTGCCTTTTGCTTTCGTTTT	
fruB-TSS-1F	GCCTGCACGCAATGCCGATG	TSS mapping
fruB-TSS-1R	TTTGCTGAATCCTTTCAGCT	
fruB-TSS-2F	TCGATTCAGTATTAAAGCTG	
fruB-TSS-2R	TCCCGTCTCGTTTTCCTTTG	
fruB-TSS-3F	AGGATTCAGCAAAAGTACCG	
fruB-TSS-3R	ATACCTTGTCATTCATCCCG	
fruB-TSS-4F	GTCAGATTGTGTCGAGTATC	
fruB-TSS-4R	TGTCTGCCTCTATAGGCGAG	
fruR-TSS-1F	GATTCAGCGTATAATTCAAC	
fruR-TSS-1R	AGCCATCACTTTGTGCTGC	
fruR-TSS-2F	GGCTAGGATCAAAAATCGCG	
fruR-TSS-2R	CCGGAAATTATACTGCTCCA	
fruR-TSS-3F	GCACATAAAACGAGACCCCC	
fruR-TSS-3R	TGCCTGCACGCAATGCCGAT	
fruB-PE(HEX)	GATACTCGACACAATCTGAC	Primer extension
fruR-PE	GATCCGATATTTCTGCGCCTTGCCG	
fruB-K-F	CCAGTGTCATAAGGGGGT CTCGTTT	$KMnO_4$ footprinting
fruB-K-R(HEX)	CAACGGTACTTTTGCTGAATCCTT	

*Engineered restriction sites were underlined with the corresponding restriction enzyme shown in parentheses

References

1. Ayala, J.C., Wang, H., Benitez, J.A. and Silva, A.J. (2018) Molecular basis for the differential expression of the global regulator VieA in *Vibrio cholerae* biotypes directed by H-NS, LeuO and quorum sensing. *Mol Microbiol*, **107**, 330-343.
2. Ryu, Y., Kim, Y.J., Kim, Y.R. and Seok, Y.J. (2012) Expression of *Vibrio vulnificus* insulin-degrading enzyme is regulated by the cAMP-CRP complex. *Microbiology*, **158**, 1294-1303.
3. Craig, M.L., Tsodikov, O.V., McQuade, K.L., Schlax, P.E., Jr., Capp, M.W., Saecker, R.M. and Record, M.T., Jr. (1998) DNA footprints of the two kinetically significant intermediates in formation of an RNA polymerase-promoter open complex: evidence that interactions with start site and downstream DNA induce sequential conformational changes in polymerase and DNA. *J Mol Biol*, **283**, 741-756.
4. Miller, V.L. and Mekalanos, J.J. (1988) A novel suicide vector and its use in construction of insertion mutations: osmoregulation of outer membrane proteins and virulence determinants in *Vibrio cholerae* requires *toxR*. *J Bacteriol*, **170**, 2575-2583.
5. Milton, D.L., O'Toole, R., Horstedt, P. and Wolf-Watz, H. (1996) Flagellin A is essential for the virulence of *Vibrio anguillarum*. *J Bacteriol*, **178**, 1310-1319.
6. Lim, J.G., Bang, Y.J. and Choi, S.H. (2014) Characterization of the *Vibrio vulnificus* 1-Cys peroxiredoxin Prx3 and regulation of its expression by the Fe-S cluster regulator IscR in response to oxidative stress and iron starvation. *J Biol Chem*, **289**, 36263-36274.
7. Chang, A.C. and Cohen, S.N. (1978) Construction and characterization of amplifiable multicopy DNA cloning vehicles derived from the P15A cryptic miniplasmid. *J Bacteriol*, **134**, 1141-1156.

8. Heo, K., Park, Y.H., Lee, K.A., Kim, J., Ham, H.I., Kim, B.G., Lee, W.J. and Seok, Y.J. (2019) Sugar-mediated regulation of a c-di-GMP phosphodiesterase in *Vibrio cholerae*. *Nat Commun*, **10**, 5358.